American Mineralogist, Volume 77, pages 329–335, 1992

Diagnostic microstructures for primary and deformational quartz rods in graphic granite

HARM STEL
Institute of Earth Sciences, Vrije Universiteit, de Boelelaan 1085, 1081 HV, Amsterdam, the Netherlands

ABSTRACT

Two varieties of quartz rods (type I and type II) that differ in microstructure and origin occur in graphic granite. Type I rods are pseudomorphous after monoclinic feldspar crystals. These are interpreted to have grown in "negative crystals" that were created during alternation of cellular and tabular growth phases. Type II rods have irregular quartz-feldspar interfaces that are located at the extensions of shear faults in the feldspar host. These quartz rods are interpreted as linear dilatational structures generated by interference of regularly spaced shear faults subparallel to crystal cleavages in feldspar. Diagnostic microstructures are parallel opposing surfaces of quartz rods, position of quartz-feldspar interfaces along shear faults, presence of quartz rods in boudin necks of retrogressive mica, and transitional relationships between graphic granite and cracked, monocrystalline feldspar domains.

INTRODUCTION

A graphic granite is an intimate intergrowth of feldspar and linear quartz rods of which cross-sectional shapes are reminiscent of (ancient) script symbols (cf. Smith and Brown, 1988). Basically, there are two models for the origin of this texture. A replacement origin of feldspar by quartz was proposed by Hutton (1788) and Drescher-Kaden (1948). Most other authors (e.g., Fersman, 1928; Černý, 1971; Fenn, 1986; Smith and Brown, 1988) maintain that graphic granites have a primary growth texture. Fenn (1986) suggested that growth of quartz takes place from SiO_2-enriched melt that is trapped in grooves that formed by alternating tabular and cellular growth stages of feldspar. Fenn's model is the present consensus (Smith and Brown, 1988).

In this paper, the model of Fenn is evaluated on the basis of a microstructural study. It is found that microstructures in specific types are consistent with Fenn's model. However, it is demonstrated that other types of graphic textures resulted from deformation of feldspar megacrystals, at which time dilatational rods formed. Material studied was sampled from pegmatite dikes of southwest Finland, specifically from the Kemiö pegmatite (Nurmi and Haapala, 1986), the Orijärvi pluton (Stel, 1991), and the Somero granite (Stel et al., 1989).

MINERAL COMPOSITION AND MICROSTRUCTURE

Graphic granites studied consist of ca. 70% alkali feldspar, 25% quartz, and minor amounts of tourmaline, mica, and chlorite. The feldspar host is microcline that has crosshatch twinning and albite lamellae. All the specimens studied contain mica aggregates that are found either as typical pegmatitic booklets of biotite and white mica or as small isolated flakes. Biotite crystals include sphene, hematite, and rutile. Invariably, mica shows alteration to chlorite and potassium feldspar intergrowths. In all the specimens, the quartz *c*-axis fabrics have single maxima.

Although graphic granites are very similar in texture, the microstructure of the quartz rods differs in detail. Two types of rods are discussed (type I and type II), for which different mechanisms of formation have been deduced. The microstructure of the two types of rods is described below.

Type I rods

Type I quartz rods are platy linear, with aspect ratios varying between 20:5:1 and 40:10:1. Cross-sectional shapes of rods are reminiscent of gothic script symbols (Fig. 1a), with concave and convex boundaries that differ consistently (cf. Drescher-Kaden, 1948). The feldspar host is monocrystalline and demonstrates excellent {001}, {010}, and {110} cleavages. Chips of 50–100 μm in thickness are easily obtained by splitting a sample along cleavage planes, allowing rapid identification of crystallographic directions. Convex quartz rod boundaries are striated pseudofaces that are exposed on cleaved fragments of hand specimen size. These boundaries are subparallel to {010}, {110}, and {1$\bar{1}$0} of the feldspar host. Consequently, convex sides of quartz rods are pseudomorphous after feldspar (Fig. 1b). Striations on convex boundaries are parallel to the intersection of the interfaces with {001} of feldspar. In type I rods, striae are sharply edged and striated surfaces are similar to stepped faces of freely grown crystals. Concave rod boundaries are highly irregular and may show interfaces with dendritic feldspar (Fig. 1a).

0003–004X/92/0304–0329$02.00

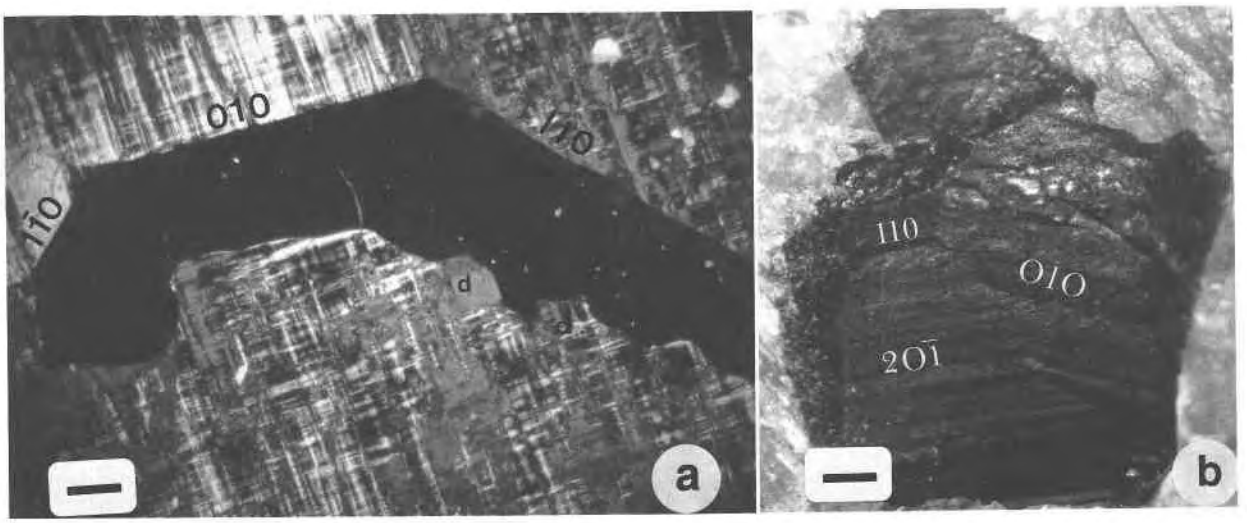

Fig. 1. (**a**) Micrograph of thin section showing cross section of type I quartz rod (dark) in twinned microcline host. Note that convex rod boundaries are straight and subparallel to crystallographic planes in the feldspar host. Concave boundary is irregularly shaped but shows occurrence of dendritic feldspar (d). Crossed polarizers. Scale bar: 0.5 mm. (**b**) Photograph of outcrop of convex side of a quartz rod in type I graphic granite. Note sharply edged steps on surfaces and pseudomorphology after feldspar morphology (indexed planes). Reflected light. Scale bar: 1 mm.

Type II rods

Type II rods are strain-free quartz crystals that occur in a strongly deformed feldspar host. The rods are regularly spaced and have aspect ratios of ca. 20:2:1. The longest axis of a rod is parallel to the intersection line of two cleavage-related cracks in the feldspar host. The spatial occurrence and shape of the rods are closely associated with deformation of the feldspar host. Microcline shows significant deformation along microscopic shear zones and faults (Fig. 2a). Cracks are heavily stained by hematite, and they are associated with local recrystallization and albite domains. Microscopic shear zones are revealed by sigmoidal bending of twin lamellae and albite strings (Fig. 2b). Some albite lamellae appear to transect microfaults. The microshear zones trend subparallel to crystal cleavages, specifically {010} and {001}, and are regularly spaced with a spacing of ca. 5 mm. Shear faults terminate at quartz-feldspar interfaces or are integrated into these. Younger cracks, which are not visibly associated with shear movement, transect all the above-mentioned structures and cross-cut both feldspar and quartz.

In cross section, the rods are rectangular, L shaped, or have an irrational outline (Fig. 2a). Inclusion trails of feldspar fragments run parallel to the longest axes of the rods (Fig. 2c). Quartz crystals include randomly oriented, nonstrained rutile needles. Quartz-feldspar interfaces always lie along more extensive shear faults in feldspar (Figs. 2a, 2b). Two types of quartz-feldspar interfaces are distinguished: (1) rough surfaces, which are morphologically similar to rupture cracks in cataclastic feldspar (Fig. 2c), and (2) smooth, naturally polished surfaces, which have rounded striae of cylindrical crests and troughs (Fig. 2d). These smooth surfaces are locally intercepted by rough, stepped albite domains (Fig. 2e) that are topographically depressed.

Opposite boundaries of some of the rods appear to be matching (Fig. 2f), i.e., they can be united by simple translation or rotation. Quartz rods transect deformed mica aggregates and are locally continuous in microboudin necks of tourmaline and biotite (Fig. 3a). In some cases, rods show a composite structure with alternating translucent and milky quartz bands (Fig. 3a).

In some specimens, graphic granite texture is transitional to monocrystalline feldspar or quartz domains, especially in domains that show heterogeneous deformation. This is illustrated in Figure 3b, which shows strongly deformed, rod-bearing feldspar in contact with a less deformed region. At the contact zone, quartz rods are in crystallographic continuity with a planar extensional quartz vein.

Occurrence of type II rods is usually associated with deformation of biotite, which shows strong alteration at kink bands and microboudin necks. Some deformed mica aggregates occur as inclusions in quartz rods (Fig. 3a).

Interpretation

The microstructures of rods in graphic granite cannot be explained by one single mechanism of formation, and it is proposed that quartz rods in graphic granite can be formed in space that was created either by deformation or by growth perturbations of the feldspar host. Both types of rods may be present in one specimen.

Type I rods

The morphology of the boundaries of type I rods is diagnostic of growth in negative feldspar. It is characterized by occurrence of striated planar pseudofaces at the

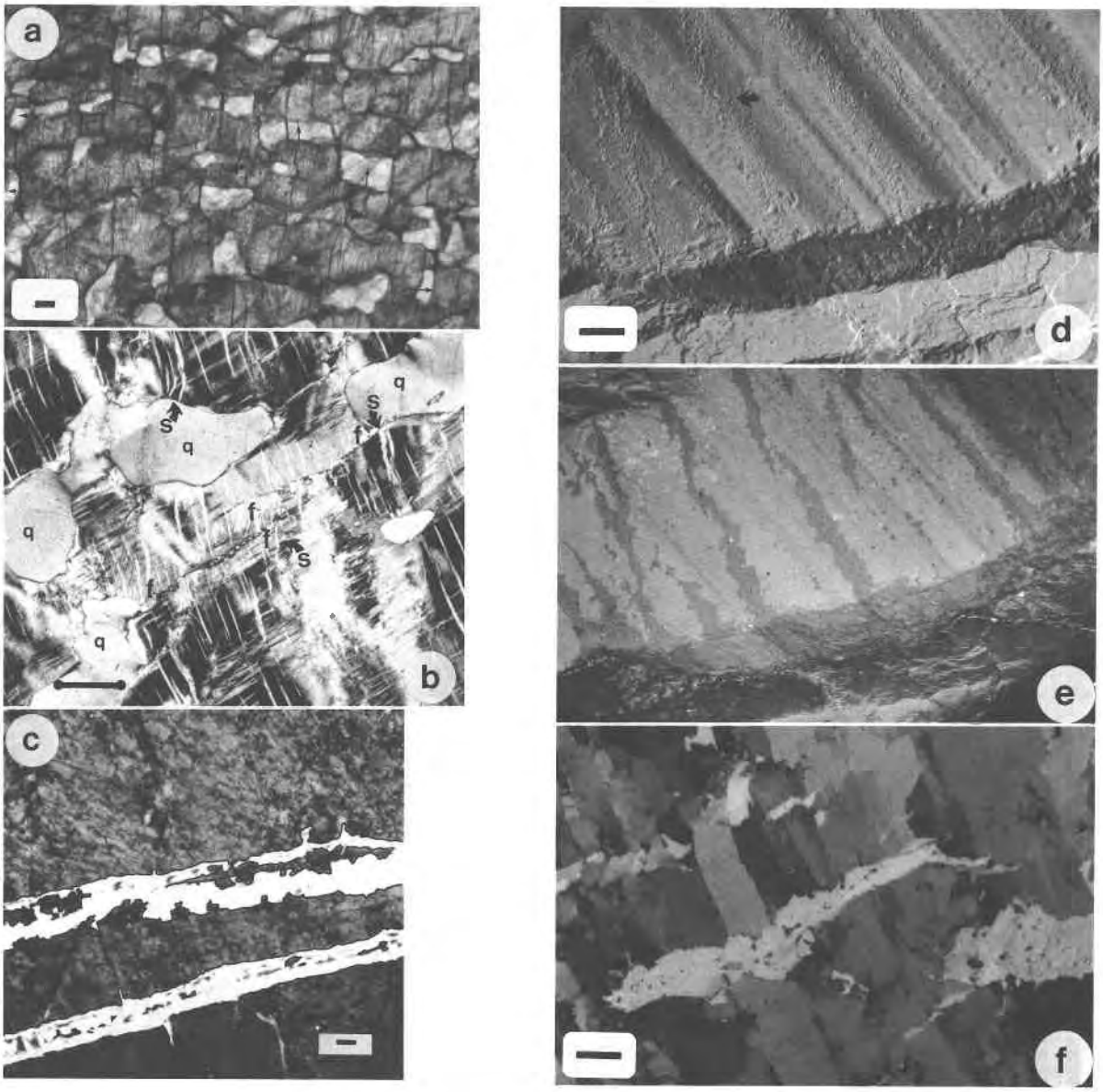

Fig. 2. (**a**) Plane-polarized-light micrograph of doubly polished section, 2 mm thick, showing cross section of optically strain-free quartz rods (white) in twinned, deformed feldspar host (gray tone). Faults run north and east and are stained with hematite and crushed particles. Note that the quartz rods are located at the intersections of faults and that quartz-feldspar interfaces are located at the extension of these faults. Note also the cross-sectional shape of the rods (predominantly rectangular; parallelism of opposite boundaries of some of the rods indicated by arrows). Scale bar: 3 mm. (**b**) Micrograph (crossed polarizers) showing microstructure of graphic granite with quartz rods (q) in feldspar host. Microshear zones and faults (marked f) in feldspar are integrated in quartz-feldspar interfaces. The feldspar host shows evidence of ductile deformation by sigmoidal bending of albite lamellae (s). Scale bar: 1 mm. (**c**) Micrograph (crossed polarizers) of a section cut parallel to type II rods. Quartz rods contain inclusion trails of feldspar; these run parallel to the rod boundary. This microstructure suggests a crack-seal origin (see text). Scale bar: 1 mm. (**d**) SEM photograph (secondary electron image) of striated fault surface of feldspar in type II graphic granite. Note the cylindrical crest and trough pattern and the smooth, polished surface, which is intercepted by rough domains (one is indicated by arrow). Scale bar: 1 mm. (**e**) SEM photograph (backscattered mode) of same surface of **d** showing that rough domains correlate with perthite strings (note that albite is dark, potassium feldspar is light). (**f**) Micrograph of type II quartz rods (white) showing rough boundaries (cf. Fig. 5f) that demonstrate a nearly perfectly fitting relationship. Crossed polarizers. Scale bar: 0.5 mm.

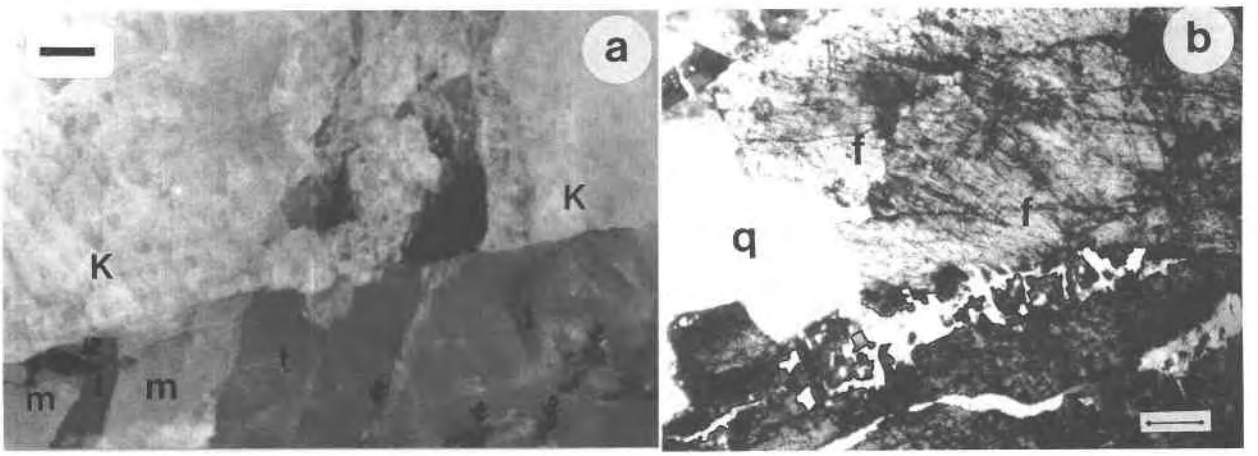

Fig. 3. (**a**) Micrograph of polished surface of type II graphic granite showing composite quartz rod structure that is built up by translucent (t) and milky quartz bands (m). Note the inclusions of deformed and boudinaged biotite inclusions (arrows). K: feldspar host. Reflected light micrograph. Scale bar: 1 mm. (**b**) Micrograph (crossed polarizers) of transition zone of graphic granite to monocrystalline quartz (q) and feldspar (f) domain. Rod-bearing feldspar is strongly deformed and appears dark because of staining of microcracks by hematite. At the transition zone to less deformed feldspar, rods are transitional to a planar extensional quartz vein (q). Scale bar: 3 mm.

convex side and dendritic interfaces at the concave side. Striated quartz rod boundaries are common to most graphic granite described in the literature, and they have been interpreted as pseudoeuhedral quartz faces (Fersman, 1928). However, there is no simple relationship between the crystallographic orientation of quartz rods and their morphology (Drescher-Kaden, 1948). On the other hand, pseudofaces and striations are subparallel to crystallographic planes {110}, {1$\bar{1}$0}, {010} and intersections of these faces with {001} of the feldspar host, respectively. Furthermore, the striated faces are morphologically similar to stepped growth surfaces of euhedral feldspar crystals. It is therefore proposed that these quartz-feldspar interfaces originated as euhedral monoclinic feldspar faces, with indices {110} and {1$\bar{1}$0}. The morphology of the quartz boundary is considered to be an imprint of this euhedral feldspar face. The morphology of the rods is fully compatible with the growth model as proposed by Fenn (1986), who suggested that quartz rods represent the infill of grooves in feldspar that formed by repeated cellular growth and subsequent tabular overgrowth (Fig. 4).

Type II rods

Type II rods are interpreted as secondary structures that were formed in dilatational sites that were created during deformation of a feldspar megacrystal. Parallelism of opposite boundaries of type II rods, and their presence in boudin necks of mica and tourmaline, demonstrates a dilatational environment (Borradaile et al., 1982, p. 26). These microstructures can hardly be explained by any other mechanism. A geometrical model of linear extensional structures has been recently proposed by Stel (1991). This model involves creation of linear dilatation structures at the intersection of two active conjugate shear faults along crystal cleavage in feldspar (Figs. 5a–5c). By this mechanism, linear dilatation structures (rods) that have a rectangular shape and matching opposite boundaries are generated. The rods occur in a regularly spaced pattern, with spacing related to that of the faults (Fig. 5c). L-shaped dilatation sites will be formed when slip on two faults is simultaneous (Fig. 5d). Irregularly shaped dilatation sites will be generated if the shear faults are nonplanar. When the amount of slip exceeds the spacing distance of the faults, linear dilatation structures become united and form planar veins (Fig. 5e). Irregularly shaped rod boundaries are created when the step-over crack is irregular (Fig. 5f). There are a number of similarities between microstructures in graphic granite and the geometry of dilatation structures such as those modeled above:

1. Quartz occurs as optically strain-free crystals in a strongly deformed feldspar host; moreover, it includes strain-free solid inclusions (notably rutile needles), which suggests that quartz is a neocrystalline phase, postdating deformation (cf. Poirier and Guiloppé, 1979).

2. One of the marked similarities is that the spacing of quartz rods in natural graphic granite obeys strict geometrical laws (Drescher-Kaden, 1948). In the model, such a spacing is a direct consequence of interference of spaced faults (cf. Figs. 2a and 5c).

3. Quartz rods in graphic granite are enclosed in a feldspar host that shows sets of shear faults parallel to cleavage directions. Quartz rods occur at intersection lines of the microfaults, and quartz-feldspar interfaces lie along these faults in a way similar to that of the model (cf. Figs. 2a and 5c).

4. The quartz rod boundaries are either striated, similar to slickenside striae (Fig. 2d), or are rough and irregular

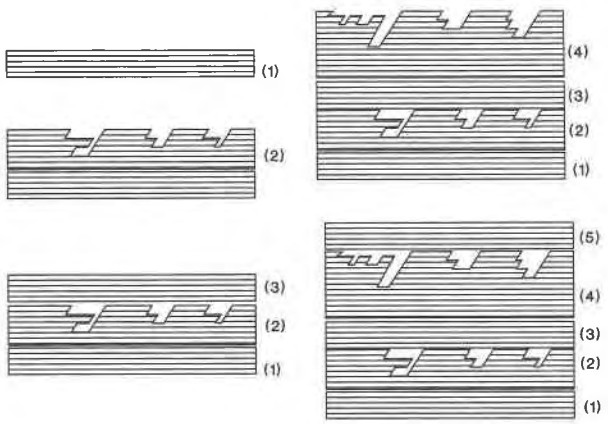

Fig. 4. Model of formation of type I rods in graphic granite by alternating tabular (1, 3, 5) and dendritic growth (2, 4) stages. Hatched = feldspar, white = grooves that are subsequently filled by quartz rods.

surfaces (Fig. 2f), similar to rupture cracks. The model predicts that a rod is bounded by two shear faults and two extensional faults which are located at the step-over. It is suggested that striated surfaces represent shear faults and rough surfaces are extensional cracks.

5. A number of rods are demonstrably linear dilatation sites, and quartz occurs as a nonstrained mineral in a sheared environment. The observed transition of planar extensional quartz veins to linear rods is as to be expected with the model (cf. Figs. 3b and 5e).

6. The texture of some rods that are built up of bands of translucent and milky quartz, with mica inclusions at the boundary, is similar to that of crack-seal veins (Ramsay, 1980). This suggests an origin by step-wise extension and subsequent healing. Also, inclusion trails that run parallel to the long axes of the rods (Fig. 2c) can be explained in this way, as crack seal veins commonly display trails of country rock fragments that were isolated by microcracking and incorporated in the vein by a subsequent healing event.

Based on the convergence of model and natural microstructures, I suggest that quartz rods in type II graphic granite are linear dilatation veins. It is clear that these rods are secondary structures, formed after growth of feldspar. The relative age of the rods with respect to other secondary structures can vary. In some cases, the deformation that caused the formation of these rods postdated the onset of exsolution of albite, as albite lamellae are sigmoidally bent in microshear zones. However, other albite lamellae transect the shear faults, suggesting prolonged exsolution that continued until a postdeformational time. The topographically depressed domains on polished fault surfaces (Figs. 2d, 2e) are also interpreted to result from postkinematic exsolution. As these depressed domains correlate with albite lamellae, they are interpreted as shrinkage structures, related to the decrease in volume of albite relative to the nonexsolved original mineral.

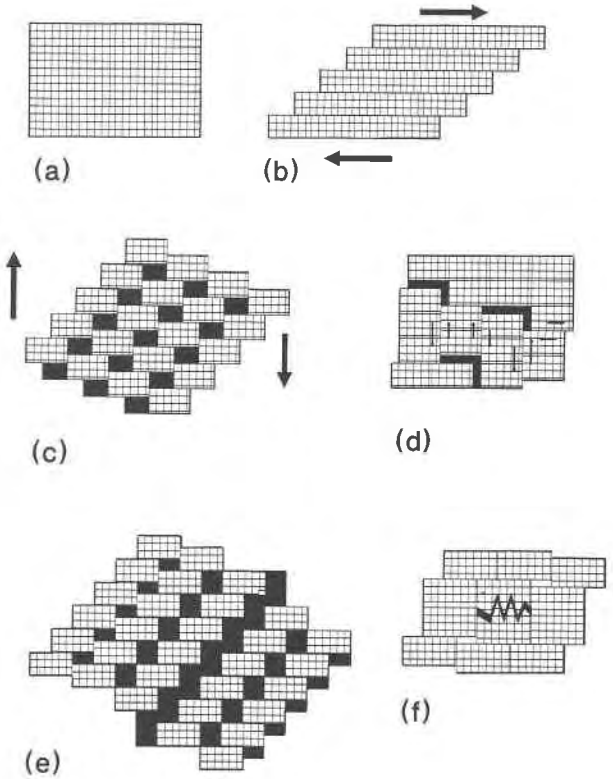

Fig. 5. Geometrical model for the formation of linear dilatation sites by interference of sets of spaced shear faults. (**a**) Nonstrained solid containing two sets of spaced discontinuities. (**b**) Slip took place along one of the sets of faults, which caused dislocation of the other. (**c**) After activation of second set of faults, spaced linear dilatation structures (black) occur at intersection lines. (**d**) L-shaped dilatation structures formed by simultaneous slip along faults. (**e**) A planar dilatation structure is formed when the amount of displacement becomes larger than the fault spacing. (**f**) Irregularly shaped dilatational structures.

Discussion and conclusions

Major points of discussion on the origin of graphic granite include the role of replacement of feldspar by quartz, the crystallographic alignment of quartz, and the chemical composition of the rocks. This microstructural study is not conclusive on these points; however some circumstantial evidence can be extracted.

1. The crystallographically controlled orientation of quartz in graphic texture remains unexplained. It is, however, noted that both types of quartz rods have similar crystallographically controlled textures.

2. No evidence was found pro or contra a replacement origin of graphic granite. In fact, no diagnostic microstructures are known to reveal this process, as in such a case it would probably involve the dissolution of feldspar and growth of quartz. However, as the rod boundaries appear to have retained fine-scale striation patterns, which can be attributed to either growth or deformation, it is unlikely that the presently discussed quartz-feldspar interfaces have been subjected to corrosion.

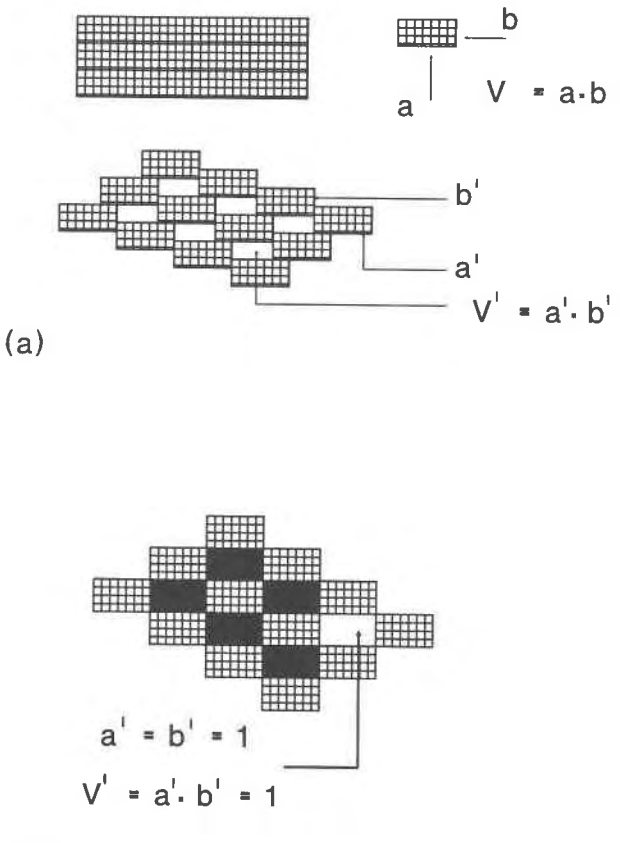

Fig. 6. Illustration of the relation of compositional variation, fault spacing, and amount of displacement. (**a**) Relation of fault spacing a and b, the feldspar block volume V, the normalized displacement a' and b', and the normalized dilatational volume V'. (**b**) Slip has reached maximum value to retain a graphic structure; $V' = 1$; if further slip would take place, planar veins would be generated (cf. Fig. 5e).

3. Graphic granite from a specific location appears to show a narrow range in composition (cf. Smith, 1974, p. 602–606), with an average quartz/feldspar ratio of 1:3, with extreme compositions having a ratio of 1:1. This has been interpreted as an argument for an origin by rapid crystallization from a melt with similar composition (Černý 1971; Fenn, 1986). Of course, a restricted chemical compositional range is not to be expected for an origin by replacement of feldspar by quartz. It is, however, important to note that a deformational origin of graphic structures will also yield a restricted compositional range, provided that deformation is homogeneous on the scale of a specimen. The model presented in this paper involves interaction of two sets of slip faults that, by mutual displacement, create linear dilatation in which quartz may crystallize. Now, the relative volume of dilatation space depends on the amount of displacement on the faults. If the spacing of the two sets of faults is a and b, respectively (Fig. 6a), the volume of the smallest rigid feldspar block that can be displaced independently is $V = a \cdot b$. The amount of slip along the faults can be expressed as the normalized displacement a' and b', which represents the ratio of the displacement and spacing of the faults (Fig. 6a). The ratio of the volume of a dilatation site and feldspar block is given by $V' = a'b'$. As the number of dilatation sites equals that of feldspar blocks, the quartz content of deformational graphic granite is given by $V'/(V' + 1)$. So V' is constant and its variation will depend only on the degree of heterogeneity of deformation. There is an upper limit for V' that is reached when $a' = b' = 1$ and that yields a quartz content of 50% (cf. Fig. 6b). A larger value of either a' or b' will yield planar extensional veins and destroy the graphic texture (cf. Fig. 5e). It is interesting to note that this upper limit matches closely that of published chemical analyses of graphic granite (Černý, 1971; Smith, 1974).

A more complicated situation occurs when slip on the spaced faults has an arbitrary value, i.e., by heterogeneous deformation. This situation requires a more extensive statistical treatment, but in the scope of this paper, a simple numerical example illustrates that deformational graphic granite should have a fixed bulk composition. Suppose that displacement took place on all spaced faults but that the amount of displacement varies arbitrarily. The maximum value of a' and b' is 1.0, and a minimum value is chosen as 0.1 (when a' or $b' = 0$, no step-over will be created). When a large number (n) of quartz rods is considered, the mean value of V', V'_m, is the product of the mean values of the normalized displacements on all the faults:

$$V'_m = (\sum_0^n V')/n = (\sum_0^n a')/n \cdot (\sum_0^n b'/n).$$

As both a' and b' vary arbitrarily between 0.1 and 1.0, $(\Sigma_0^n a')/n = (\Sigma_0^n b'/n) = 0.55$, and $V'_m = 0.3025$. This corresponds with a relative quartz volume of 23%. This value correlates remarkably well with chemical analyses in the literature (cf. Smith, 1974, p. 603).

This discussion is not meant to imply that graphic granite in general has a deformational origin, but it does show that occurrence of restricted compositional variations alone is not conclusive for a crystallization origin.

In conclusion, microstructures in graphic granite are consistent with two models of formation: by crystallization perturbations or by dilatational deformation. The discrimination between either mechanism can be readily performed by applying diagnostic microstructural criteria such as given in this paper.

Acknowledgments

SEM analyses were performed by Saskia Kars from the Micro Analyse Laboratorium, VU Amsterdam. Randall Stephenson corrected earlier versions of the manuscript. P. Fenn and T. McCormick gave valuable suggestions for improvement of the manuscript.

References cited

Borradaile, G.J., Bayly, M.B., and Powell, C.McA. (1982) Atlas of deformational and metamorphic rock fabrics, 551 p. Springer-Verlag, Berlin.

Černý, P. (1971) Graphic intergrowths of feldspars and quartz in some Czechoslovak pegmatites. Contributions to Mineralogy and Petrology, 30, 343–355.

Drescher-Kaden, F.K. (1948) Die Feldspat-Quartz Reaktionsgefüge der Granite und Gneise, 259 p. Springer-Verlag, Berlin.

Fenn, P.M. (1986) On the origin of graphic granite. American Mineralogist, 71, 325–330.

Fersman, A.E. (1928) Die Schriftstruktur der Granit-Pegmatite und ihre Entstehung. Zeitschrift für Kristallographie, 69, 77.

Hutton, J. (1788) Theory of the Earth, 620 p. (reprinted 1959). Royal Society Edinburgh, Edinburgh.

Nurmi, P.A., and Haapala, I. (1986) The Proterozoic granitoids of Finland: Granite types, metallogeny and relation to crustal evolution. Bulletin of the Geological Society of Finland, 58, 203–233.

Poirier, J.P., and Guiloppé, M. (1979) Deformation induced recrystallization of minerals. Bulletin de Minéralogie, 102, 67–74.

Ramsay, J.G. (1980) The crack-seal mechanisms of rock deformation. Nature, 284, 135–139.

Smith, J.V. (1974) The feldspars, vol. 2, 690 p. Springer-Verlag, New York.

Smith, J.V., and Brown, W.L. (1988) Feldspar minerals, 828 p. Springer-Verlag, New York.

Stel, H. (1991) Linear dilatation structures and syn-magmatic folding in granitoids. Journal of Structural Geology, 13, 625–634.

Stel, H., Veenhof, J., Huizenga, J.M., Timmerman, M., and Hartsink, J.M.H. (1989) Infra-supra structure relations of a microcline granite dome in the Somero area, Svecofennides, SW Finland. Bulletin of the Geological Society of Finland, 61, 131–141.

Manuscript received March 5, 1991
Manuscript accepted November 4, 1991